

QCD running in neutrinoless double beta decay: Short-range mechanisms

M. González* and S.G. Kovalenko†

*Universidad Técnica Federico Santa María,
Centro-Científico-Tecnológico de Valparaíso,
Casilla 110-V, Valparaíso, Chile*

M. Hirsch‡

*AHEP Group, Instituto de Física Corpuscular – CSIC./Universitat de València
Edificio de Institutos de Paterna, Apartado 22085, E-46071 València, Spain*

Abstract

The decay rate of neutrinoless double beta ($0\nu\beta\beta$) decay contains terms from heavy particle exchange, which lead to dimension-9 ($d = 9$) six fermion operators at low energies. Limits on the coefficients of these operators have been derived previously neglecting the running of the operators between the high-scale, where they are generated, and the energy scale of $0\nu\beta\beta$ -decay, where they are measured. Here we calculate the leading order QCD corrections to all possible $d = 9$ operators contributing to the $0\nu\beta\beta$ amplitude and use RGE running to calculate 1-loop improved limits. Numerically, QCD running dramatically changes some limits by factors of the order of or larger than typical uncertainties in nuclear matrix element calculations. For some specific cases, operator mixing in the running changes limits even by up to three orders of magnitude. Our results can be straightforwardly combined with new experimental limits or improved nuclear matrix element calculations to re-derive updated limits on all short-range contributions to $0\nu\beta\beta$ decay.

Keywords: double beta decay, physics beyond the standard model, neutrinos

*Electronic address: marcela.gonzalezp@usm.cl

†Electronic address: sergey.kovalenko@usm.cl

‡Electronic address: mahirsch@ific.uv.es

I. INTRODUCTION

Non-observation of neutrinoless double beta ($0\nu\beta\beta$) decay constrains lepton number violating extensions of the Standard Model (SM). Usually lower limits on $0\nu\beta\beta$ decay half-lives are interpreted as upper limits on the effective Majorana neutrino mass, $\langle m_\nu \rangle = \sum_j m_j U_{ej}^2$, but many models generating a non-zero $0\nu\beta\beta$ decay amplitude not directly proportional to $\langle m_\nu \rangle$ have been discussed in the literature, for recent reviews on $0\nu\beta\beta$ decay see for example [1, 2].

One can classify the different contributions to the general $0\nu\beta\beta$ decay rate either as long-range [3] or as short-range [4] contributions. The long-range part of the amplitude describes the exchange of a light neutrino between two point-like vertices. If both vertices are the SM charged current vertices, the resulting diagram corresponds to the well-known mass mechanism, but other long range contributions, not directly proportional to $\langle m_\nu \rangle$, do exist in many models, like for example R-parity violating SUSY [5–7] or leptoquark models [8].

The short-range part of the $0\nu\beta\beta$ amplitude is due to “heavy” particle exchange.¹ After integrating them out the amplitude can be represented as (the nuclear matrix element of) a true dimension-9 ($d = 9$) quark-level effective operator, which can be schematically written as:

$$\mathcal{O}_{d=9} \propto \frac{1}{\Lambda_{\text{LNV}}^5} \bar{u}\bar{u} dd \bar{e}\bar{e} . \quad (1)$$

The general $SU(3)_c \times SU(2)_L \times U(1)_Y$ invariant decomposition of this $d = 9$ operator has been discussed in [9]. The tables given in [9] can be understood as a summary of all (proto-) high-energy scale models, which contribute to $0\nu\beta\beta$ decay at tree-level via heavy particle exchange. Once all possible ultraviolet (UV) completions of Eq. (1) have been specified, one can then use the results of [4] to derive general limits on all possible models contributing to $0\nu\beta\beta$ decay.

Given current experimental lower limits on half-lives of $0\nu\beta\beta$ decay, of the order of (few) 10^{25} ys for ^{76}Ge [10] and ^{136}Xe [11–13], the energy scale, Λ_{LNV} , at which the effective interactions (1) are generated, is expected to be of the order of roughly $\mathcal{O}(\text{TeV})$. On the other hand, $0\nu\beta\beta$ decay is a low-energy process with the typical momentum scale given by the Fermi momentum of nucleons, $p_F \sim 100$ MeV. This rather large mismatch in scales implies that the running of the operators under the renormalization may be quite important numerically. This observation forms the basic motivation for the current paper.

The Operator Product Expansion (OPE) and the renormalization group equation (RGE) have become the standard tool [14, 15] in electro-weak precision physics. Here, we extend this formalism to $0\nu\beta\beta$ -decay. We shall specify all possible $d = 9$ operators contributing to $0\nu\beta\beta$ decay and calculate their QCD leading order RGE running. Color mismatched operators, which appear in this calculation, lead to operator mixing. Since different operators in $0\nu\beta\beta$

¹ Any particle with mass larger than the typical Fermi momentum of the nucleons, i.e. $\mathcal{O}(0.1)$ GeV, can be considered “heavy” in $0\nu\beta\beta$ decay. All exotic fermions contributing to the short-range amplitude, except possibly sterile neutrinos, are expected to have masses larger than $\mathcal{O}(100)$ GeV.

decay can have vastly different nuclear matrix elements, this effect in some case leads to a rather drastic change in the derived limits. It is therefore important to take these QCD corrections into account in the calculation of limits on short-range operators.

We note, that our paper is not the first to consider QCD corrections. In [16] the author observed that the color mismatch generated by the QCD corrections is expected to be important in the case of the scalar-pseudoscalar quark operators (\mathcal{O}_1 in the notations of Eq. (3)). Reference [17] treats in details the running and mixing of the scalar-pseudoscalar and tensor operators ($\mathcal{O}_{1,2}^{RR}$ in the notations of Eqs. (3)-(4)). Our current paper, however, is the first one to give the leading order QCD corrections to the complete set of the short-range $d = 9$ $0\nu\beta\beta$ -operators covering the low-energy limits of any possible underlying high-energy scale model.

The rest of this paper is organized as follows. In the next section we remind the most important definitions for operators, currents and the $0\nu\beta\beta$ -decay half-life given in [4], before summarizing in section III how to connect low-energy $0\nu\beta\beta$ -decay with the possible ultra-violet completions (“models”) of the $d = 9$ operators [9]. Section IV describes the formalism of effective theories based on the operator product expansion and the renormalization group, which we use in the analysis of $0\nu\beta\beta$ -decay. Section V contains the central result of the present paper: the leading order *QCD corrected $0\nu\beta\beta$ -decay half-life formula* (45). Here we also discuss our numerical results, before closing with a short summary in section VI.

II. LOW-ENERGY EFFECTIVE LAGRANGIAN AND $0\nu\beta\beta$ -DECAY HALF-LIFE

From the low-energy point of view, adequate for the energy scale $\mu \sim 100$ MeV of $0\nu\beta\beta$ -decay, the short range (SR) part of the decay amplitude can be derived from the generic effective Lagrangian [4]²

$$\mathcal{L}_{\text{eff}}^{0\nu\beta\beta} = \frac{G_F^2}{2m_p} \sum_{i,XY} C_i^{XY}(\mu) \cdot \mathcal{O}_i^{XY}(\mu), \quad (2)$$

with the $d = 9$ operator basis containing the following complete set of Fierz non-equivalent operators, classified by their Lorentz structure:

$$\mathcal{O}_1^{XY} = 4(\bar{u}P_X d)(\bar{u}P_Y d) \ j, \quad (3)$$

$$\mathcal{O}_2^{XX} = 4(\bar{u}\sigma^{\mu\nu}P_X d)(\bar{u}\sigma_{\mu\nu}P_X d) \ j, \quad (4)$$

$$\mathcal{O}_3^{XY} = 4(\bar{u}\gamma^\mu P_X d)(\bar{u}\gamma_\mu P_Y d) \ j, \quad (5)$$

$$\mathcal{O}_4^{XY} = 4(\bar{u}\gamma^\mu P_X d)(\bar{u}\sigma_{\mu\nu}P_Y d) \ j^\nu, \quad (6)$$

$$\mathcal{O}_5^{XY} = 4(\bar{u}\gamma^\mu P_X d)(\bar{u}P_Y d) \ j_\mu \quad (7)$$

with $X, Y = L, R$ and the leptonic currents are

$$j = \bar{e}(1 \pm \gamma_5)e^c, \quad j_\mu = \bar{e}\gamma_\mu\gamma_5e^c. \quad (8)$$

² In [4] the coefficients in Eq. (2) were denoted as ϵ_i^{XY} .

Let us stress that the so-called color mismatched operators appearing in low-energy limit of high-scale models as well as due to the QCD corrections, as explained in sec. IV, can all be expressed in terms of the color-singlet operator basis (3)-(7). An example of a color mismatched operator and its expression in terms of this operator basis is given in Eqs. (15), (16).

The following notes on the effective Lagrangian (2) and the operator basis (3)-(7) are also in order. The leptonic currents $\bar{e}\gamma^\mu e^c$, $\bar{e}\sigma^{\mu\nu}e^c$ and $\bar{e}\sigma^{\mu\nu}\gamma_5 e^c$ vanish identically. That is why they do not appear in Eqs. (3)-(8). For the current $j = \bar{e}(1 \pm \gamma_5)e^c$ in Eq. (8) we used notation without distinguishing the relative sign. This is because the $0\nu\beta\beta$ -decay half-life, given below in Eq. (9), does not depend on it. Note further that the factor $\frac{G_F^2}{2m_p}$ in Eq. (2) has been chosen to make the coefficients C_i dimensionless quantities and we have introduced a factor of 4 in Eqs. (3)-(7), such that the numerical values of C_i can be directly compared with the numbers given in the original paper [4]. Finally, all the operators (3)-(7) can have superscripts XY with the exception of \mathcal{O}_2^{XX} , for which $\mathcal{O}_2^{LR} = \mathcal{O}_2^{RL} \equiv 0$.

Eq. (2) is nothing but the most general parametrization of the effective Lagrangian in terms of the quark-lepton operators of the lowest dimension, $d = 9$, which can contribute to the $0\nu\beta\beta$ -decay amplitude at tree level. No particular physics underlying the Lagrangian (2) is implied at this stage. Note that the Lagrangian (2) is tied to the typical energy scale μ of the process in question. For $0\nu\beta\beta$ -decay it is of the order of the Fermi momentum of nucleons and quarks in $0\nu\beta\beta$ -decaying nucleus, $\mu \sim p_F \sim 100$ MeV. The Lagrangian (2) can be applied to a processes with any hadronic states: quarks, mesons, nucleons, other baryons and nuclei. The corresponding amplitude is determined by the hadronic matrix elements of the operators \mathcal{O}_i of in Eqs. (3)-(7). The coefficients C_i are independent of the low-energy scale non-perturbative hadronic dynamics. This is the well-recognizable feature of the Operator Product Expansion (OPE), representing interactions of some high-scale renormalizable model in the form of Eq. (2) below a certain scale μ . The coefficients C_i are known as Wilson coefficients, depending on the parameters of a high-scale model.

Applying the standard nuclear theory methods [18], one finds for the $0\nu\beta\beta$ half-life:

$$\left[T_{1/2}^{0\nu\beta\beta}\right]^{-1} = G_1 \left| \sum_{i=1}^3 C_i(\mu_0) \mathcal{M}_i \right|^2 + G_2 \left| \sum_{i=4}^5 C_i(\mu_0) \mathcal{M}_i \right|^2 \quad (9)$$

Here, $G_1 = G_{01}$ and $G_2 = (m_e R)^2 G_{09}/8$ are phase space factors in the convention of [18]. Their numerical values for various isotopes can be found in Ref. [2]. The quantities $\mathcal{M}_i = \langle A_f | \mathcal{O}_i^h | A_i \rangle$ are the nuclear matrix elements defined in Ref. [4]. In the above equation the summation over the coefficients corresponding to the operators \mathcal{O}_i^{XY} with different chiralities $X, Y = L, R$ is implied. The Wilson coefficients $C_i(\mu_0)$ should be taken close to the typical $0\nu\beta\beta$ -energy scale. In our analysis we choose $\mu_0 = 1\text{GeV}$. In Eq. (9) we have not included interference terms, since none of the high-scale models listed in [9] mixes the coefficients $C_{1,2,3}$ with $C_{4,5}$.

Numerical values for the nuclear matrix elements \mathcal{M}_i , based on the pn-QRPA approach of [19], can be found for ${}^{76}\text{Ge}$ in [4], for other isotopes of interest see [2]. It is, however, well-known that nuclear matrix elements for $0\nu\beta\beta$ -decay have quite large numerical uncertainties.

Recent publications calculating matrix elements for heavy neutrino exchange, i.e. matrix elements for the short-range part of the amplitude corresponding in our notation to the term C_3^{LL} , give numerical values which are larger than those of [2] by typically 50 % (40 %) in the QRPA calculation by the Tübingen group [20] (Jyväskylä group [21]). Shell model calculations for light neutrino exchange, on the other hand, seem to give matrix elements which are up to a factor of two smaller than those of QRPA [22]. Similar factors are found for heavy neutrino exchange in the shell model calculation of [23]. However, a recent shell model calculation for ^{76}Ge gives matrix elements for light neutrino exchange [24] only 15-40 % smaller than those of [19]. While these variations in numerical results do probably not cover the error bar in the calculation of nuclear matrix elements completely, from these numbers one may estimate that currently matrix elements for the short-range part have uncertainties of roughly a factor of 2 or so.

We note, however, that while we do use the numerical values of [2] for the derivation of new limits, all our calculations are presented in such a way that the running of the operators is separated completely from the nuclear structure part of the calculation. Thus, our coefficients can be combined with any new nuclear matrix element calculations, should they become available, to extract updated limits. For the time being the numerical values for nuclear matrix of the whole set of the basis operators in Eqs. (3)-(7) are not available in the literature in the approaches other than that of Refs. [2, 4]. However, we have recently learned [25] that the corresponding results within the QRPA approach of the Tübingen group will be published soon.

III. LINK TO HIGH-SCALE MODELS

As already mentioned above, Eq. (2) is a general parametrization of all the possible $d = 9$ contact interactions contributing to $0\nu\beta\beta$ -decay amplitude at tree level, without referring to any underlying physics. The latter is typically thought to be represented by renormalizable models with heavy degrees of freedom which decouple from the light sector at certain energy scale (much) larger than the characteristic scale of $0\nu\beta\beta$ -decay. In the literature one can find two approaches connecting the effective Lagrangian (2) to such high-energy models. We will discuss them briefly.

Historically, the first approach was the top-down approach: Starting from a concrete high-scale model and integrating out heavy degrees of freedom of a mass M_h at energy-scales $\mu < M_h$. Then, there appear effective non-renormalizable interactions of the light fields in the form of an expansion in the inverse powers of M_h , which is the operator product expansion. The interactions (2) are then the leading $d = 9$ terms of this expansion. The well-known and simplest example of such a model is the SM, extended by a heavy Majorana neutrino N with the mass $M_N \gg \mu \sim p_F \sim 100$ MeV. The relevant Lagrangian term is

$$\mathcal{L}_{\text{SMN}} = \frac{g_2}{\sqrt{2}} \bar{e}_L \gamma^\mu U_{eN} N \cdot W_\mu^- \quad (10)$$

where g_2 is the $SU(2)_L$ gauge coupling constant and U_{eN} describes the mixing of this heavy

state with the ordinary electron neutrino. The tree-level diagram contributing to the $0\nu\beta\beta$ amplitude is shown in Fig. (1) on the left with W^\pm denoted by dashed lines. At momenta p of the external legs below both M_W and M_N one can expand the corresponding propagators in p^2/M_i^2 with $i = W, N$. The leading term is

$$\mathcal{L}_{SMN}^{\text{eff}} = -8 \frac{G_F U_{eN}}{\sqrt{2} M_N} \bar{u}_L \gamma_\mu d_L \cdot \bar{u}_L \gamma_\mu d_L \cdot \bar{e} P_R e^c. \quad (11)$$

In the path integral approach the described procedure is equivalent to integrating out the W and N fields, which consists of neglecting their kinetic terms, justified at energies below their masses, and the subsequent Gaussian integration over W and N variables. (For a pedagogical review see Refs. [14, 15]). In the literature a great host of high-scale models have been linked to the form of the Lagrangian (2) in this way. The key point here is that there are at least two orders of magnitude of hierarchy between the scale where the new degrees of freedom are integrated out and the scale of $0\nu\beta\beta$ -decay, which the parameterization of Eq. (2) is tied to. As has been pointed out for the first time in Ref. [16] in the presence of QCD loop corrections such a scale hierarchy has a significant impact on the relation of the parameters of high-scale models and the parameters C_i extracted from the measurements of $0\nu\beta\beta$ -decay half-life on the basis of Eq. (9).

Recently, a bottom-up approach to “deconstructing” $0\nu\beta\beta$ -decay has been proposed in Ref. [9]. This approach surveys in a generic way all possible renormalizable $SU(3)_c \times SU(2)_L \times U(1)_Y$ invariant interactions leading in the low energy limit to the effective operators in Eqs. (2)-(7). As demonstrated in [9], there are only two tree-level topologies for the renormalizable decompositions of these operators. These are shown in Fig. 1 and denoted T-I and T-II. The six outside lines stand for any of \bar{u} , d or \bar{e} . Dashed lines are for bosons (either scalars or vectors), the solid (inner) line in T-I is for some exotic (i.e. non-standard model) fermion. The task of defining all possible ultraviolet completions (“models”) contributing to the $0\nu\beta\beta$ -decay rate (at tree-level), then reduces the problem to finding all SM-invariant fermion bilinears involving the quarks and leptons (plus all bilinears involving one SM fermion and one exotic fermion in case of T-I) of Eq. (1) and, after integrating out all heavy (i.e. beyond SM) particles, rewrite the resulting expressions into the basis operators of Eq. (2).

To make contact with some of the known in the literature mechanisms of $0\nu\beta\beta$ -decay and to the general treatment of all the possible short range mechanisms [9], we discuss here a simple example model based on the decomposition T-I-1-i in the notations of Ref. [9]. This corresponds to the external legs in Fig. 1 (left) grouped as $(\bar{u}_L d_R)(\bar{e}_L)(\bar{e}_L)(\bar{u}_L d_R)$, so that the fields within the same parenthesis meet in the same vertex. With this choice, the two scalars $S_1 = S_2$ are fixed to be either $S_{1,2,1/2}$ or $S_{8,2,1/2}$. For the former the intermediate fermion is either $\psi_{1,1,0}$ or $\psi_{1,3,0}$, while for the latter it is either $\psi_{8,1,0}$ or $\psi_{8,3,0}$. This model partially covers the well known case of the R-parity violating SUSY mechanism [8] identifying $S_{1,2,1/2} \equiv \tilde{L}$ and $\psi_{1,1,0} \equiv \chi_0$ with $\tilde{L} = (\tilde{\nu}, \tilde{e})_L$ and χ_0 being the slepton electroweak doublet, scalar superpartner of the left-handed lepton doublet, and the neutralino, respectively. Conventionally, the subscripts denote the field assignment to certain representation of the SM

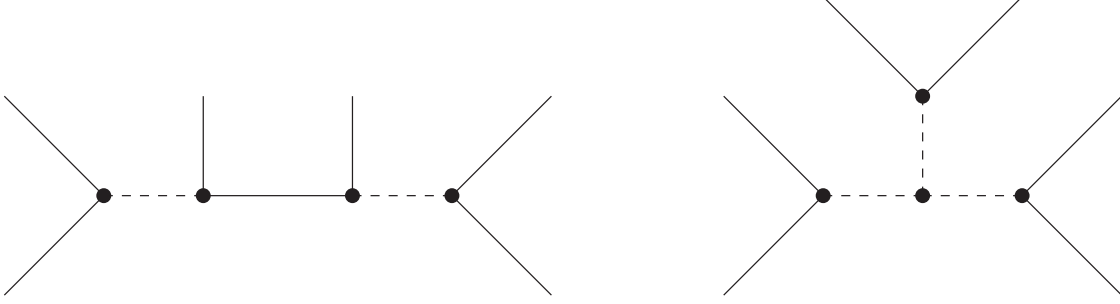


FIG. 1: Tree-level topologies contributing to the $0\nu\beta\beta$ -decay rate. To the left T-I, scalar-fermion-scalar exchange; to the right T-II, scalar-scalar-scalar diagrams. Scalars could also be replaced by vectors.

gauge group $SU(3)_c \times SU(2)_L \times U(1)_Y$ in the format (dimension, dimension, $U(1)_Y$ -charge). The model interactions appearing in the diagram T-I in Fig. 1 (left) are then given by:

$$\begin{aligned} \mathcal{L}_Y = & Y_{Qd(1)}(\bar{Q}d_R)S_{1,2,1/2} + Y_{Qd(8)}\left(\bar{Q}\frac{\lambda^A}{2}d_R\right)S_{8,2,1/2}^A \\ & + Y_{e\psi(1)}(\bar{e}_L\psi_{1,X,0})S_{1,2,1/2}^\dagger + Y_{e^c\psi(1)}(\bar{e}_L^c\psi_{1,X,0})S_{1,2,1/2} \\ & + Y_{e\psi(8)}(\bar{e}_L\psi_{8,X,0}^A)S_{8,2,1/2}^{A\dagger} + Y_{e^c\psi(8)}(\bar{e}_L^c\psi_{8,X,0}^A)S_{8,2,1/2}^A. \end{aligned} \quad (12)$$

Here, (λ^A) are the Gell-Mann matrices, and Y some unknown Yukawa couplings. Eq. (12), together with the Majorana propagator for $\psi_{C,X,0}$ and after integrating out heavy particles, gives an effective Lagrangian, which for the color octet case, $S_{8,2,1/2}$, reads

$$\mathcal{L}_{eff} = \frac{Y_{Qd(8)}^2 Y_{e\psi(8)} Y_{e^c\psi(8)}}{m_{S_{8,2,1/2}}^4 m_{\psi_{8,X,0}}} (\lambda^A/2)_a^b (\lambda^A/2)_c^d (\bar{Q}^a d_{R,b}) (\bar{Q}^c d_{R,d}) (\bar{e} P_R e^c). \quad (13)$$

The Lagrangian for the color singlet case is identical to Eq. (13) after some obvious replacements, i.e. $(\lambda^A/2)_j^i \rightarrow 1$ etc. It is also already in the basis defined in Eq. (2), so for the color-singlet case only

$$C_1^{RR} = \left(\frac{2m_p}{G_F^2}\right) \frac{Y_{Qd(1)}^2 Y_{e\psi(1)} Y_{e^c\psi(1)}}{m_{S_{1,2,1/2}}^4 m_{\psi_{1,X,0}}} \equiv C_{1(0)}^{RR} \quad (14)$$

is non-zero. For the color octet, however, before applying the standard non-relativistic impulse approximation to convert quark to nucleon currents, first the color singlet has to be extracted. Using

$$(\lambda^A)_b^a (\lambda^A)_d^c = -\frac{2}{3} \delta_b^a \delta_d^c + 2\delta_d^a \delta_b^c,$$

this leads to an operator, which contains the original operator plus a color mismatched piece:

$$-\frac{2}{3} (\bar{Q}^a d_{R,a}) (\bar{Q}^a d_{R,a}) + 2 (\bar{Q}^a d_{R,b}) (\bar{Q}^b d_{R,a}). \quad (15)$$

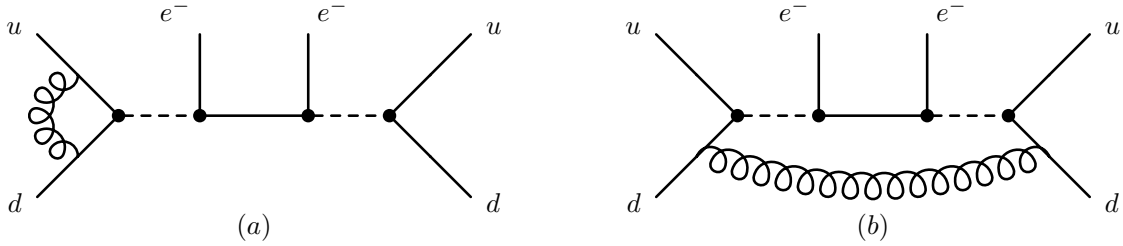


FIG. 2: $0\nu\beta\beta$ -decay example diagrams of one-loop QCD corrections to the “full theory”

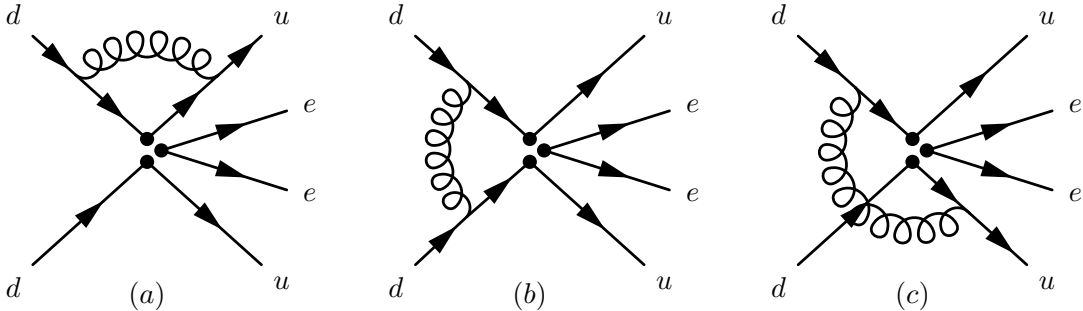


FIG. 3: One-loop QCD corrections to the short range mechanisms of $0\nu\beta\beta$ -decay in the effective theory.

This can be brought to canonical form of Eqs. (3)-(7) using Fierz rearrangement for the second mismatched term. Then we have

$$\mathcal{L}_{eff} \propto -C_1^{RR} \cdot \mathcal{O}_1^{RR} - C_2^{RR} \cdot \mathcal{O}_2^{RR}, \quad (16)$$

with

$$C_1^{RR} = \frac{5}{3}C_{1(0)}^{RR}, \quad C_2^{RR} = \frac{1}{4}C_{1(0)}^{RR}, \quad \text{and} \quad C_2^{RR} = \frac{3}{20}C_1^{RR}. \quad (17)$$

Thus there appear simultaneously two operators the \mathcal{O}_1^{RR} and \mathcal{O}_2^{RR} at the decoupling scale of the heavy fields S and ψ . In the next sections we will call this scale the matching scale Λ where we match a high-energy “full theory” with its effective low-energy theory. At the end of section V we discuss the issues of the simultaneous presence of two or more operators at the matching scale. Note that all high-energy scale models specified in Ref. [9] lead to at most two different operators in effective theory at the matching scale.

IV. OPE AND QCD EFFECTS

In this section we develop the formalism for taking into account the Leading Order (LO) QCD corrections to the operator product expansion given in Eq. (2). We follow essentially the methods described in the reviews [14, 15] for semi-leptonic and hadronic decays of mesons. An important feature of the effective Lagrangian (2), is that it involves the complete

set of $d = 9$ operators (3)-(7) contributing to $0\nu\beta\beta$ -decay. Therefore, no new operators are generated under renormalization.

A. Matching of Full Theory onto Effective One

We start with the discussion of the procedure relating the high-scale renormalizable model, typically dubbed in the present context as a “full theory”, to an effective theory represented by the Lagrangian (2) treated as the low-energy limit of the full theory. This matching procedure allows one to derive the coefficients C_i in terms of the parameters of a high-scale model and take into account the corresponding perturbative QCD effects. The matching is settled at the level of amplitudes of the full theory \mathcal{A}_{full} and of the effective one $\mathcal{A}_{eff} \sim \langle \mathcal{L}_{eff}^{0\nu\beta\beta} \rangle$ requiring they coincide

$$\mathcal{A}_{full} = \mathcal{A}_{eff} = \frac{G_F^2}{2m_p} \sum_i C_i(\mu) \cdot \langle \mathcal{O}_i(\mu) \rangle \quad (18)$$

at an energy scale $\mu \leq \Lambda$ below the heavy particle masses of the full theory. This is the so-called matching condition. In the right-hand side of this equation only the leading term $\sim (1/\Lambda)^5$ of the low-energy expansion is retained. The brackets $\langle \rangle$ denote matrix elements between the hadronic states. Since the coefficients C_i we are interested in, do not depend on the external states one can use the simplest hadronic states for the amplitude calculation, which are the quarks. For the same reason we are allowed to set quark masses to zero and assign to all of them the common value of the space-like momentum $p^2 < 0$. The latter allows us to avoid infrared singularities in the calculation. The diagrams representing the one-loop QCD corrections to the matrix elements of the effective operators in Eq. (18) are shown in Fig 3. In Fig. 2 we give an example of the set of one-loop diagrams relevant for the calculation of the full theory amplitude. In order to tackle the ultraviolet (UV) divergencies we use the dimensional regularization and the $\overline{\text{MS}}$ subtraction scheme. For simplicity we assume that the masses of all the heavy particles of the full theory are equal to a common scale $\Lambda = \Lambda_{LNV}$. Note, however, that given current LHC constraints, lower limits on Λ_{LNV} are already of the order of $\Lambda_{LNV} \sim \mathcal{O}(1)$ TeV. We will come back to this point in section V. A straightforward calculation shows the general structure of the amplitude and the operator matrix elements in the LO of the QCD perturbation theory has the following form:

$$\mathcal{A}^{Full} = \frac{g_{full}}{\Lambda^5} a_i \left[1 + c_i \frac{\alpha_s}{4\pi} \left(\frac{1}{\epsilon} + \ln \left(\frac{\mu^2}{-p^2} \right) \right) + \frac{\alpha_s}{4\pi} z_i \ln \left(\frac{\Lambda^2}{-p^2} \right) \right] \langle \mathcal{O}_i \rangle_{\text{tree}} \quad (19)$$

$$\langle \mathcal{O}_i \rangle^{(0)} = \left[\delta_{ij} + \frac{\alpha_s}{4\pi} b_{ij} \left(\frac{1}{\epsilon} + \ln \left(\frac{\mu^2}{-p^2} \right) \right) \right] \langle \mathcal{O}_j \rangle_{\text{tree}}. \quad (20)$$

Here, $\langle \mathcal{O}_i \rangle_{\text{tree}}$ are the operator matrix elements without QCD corrections. The explicit form of the matrix b_{ij} will be given in the LO approximation below. On the other hand, we do not need any knowledge of the coefficients a_i , c_i or z_i since our goal is to calculate the QCD

running of the Wilson coefficients of the effective operators, which is determined, as discussed below, by b_{ij} only. The above expression (19) is given in order to clarify some aspects of the matching. The singular $1/\epsilon$ term in Eq. (19) originates from the diagram with the vertex correction Fig. (2a), which is UV divergent, while the diagram Fig. (2b) leads to the finite second term due to the propagators of the virtual heavy particles of the mass $\sim \Lambda$ cutting the logarithmic divergence at Λ . The singularity from the first term can be eliminated by coupling constant and quark field renormalization. The quark field renormalization due to the QCD corrections is given by

$$q^{(0)} = Z_q^{1/2} q, \quad \text{with} \quad Z_q = 1 - C_F \frac{\alpha_s}{4\pi} \frac{1}{\epsilon} + O(\alpha_s^2), \quad (21)$$

where $q^{(0)}$ and q are the bare and renormalized quark fields with the renormalization constant Z_q given in the LO approximation. Here $C_F = (N^2 - 1)/(2N)$ is the standard $SU(N)$ color factor. In the case of the operator matrix elements in Eq. (20) the $1/\epsilon$ -singularities are removed by the quark field renormalization, Eq. (21), accompanied by renormalization of the operators $\mathcal{O}_i^{(0)} = Z_{ij} \mathcal{O}_j$, mixing them within certain groups of the complete list (3)-(7). These groups are identified in the next section. The operator matrix elements in Eq. (20) are renormalized as amputated Green functions

$$\langle \mathcal{O}_i \rangle^{(0)} = Z_q^{-2} Z_{ij} \langle \mathcal{O}_j \rangle. \quad (22)$$

Requiring the cancelation of the singularities in Eq. (20) one finds

$$Z_{ij} = \delta_{ij} + \frac{\alpha_s}{4\pi} (b_{ij} - 2C_F \delta_{ij}) \frac{1}{\epsilon} + O(\alpha_s^2). \quad (23)$$

The renormalized matrix elements $\langle \mathcal{O}_j \rangle$ and the amplitude \mathcal{A}^{Full} have the same form as in Eqs. (20), (19), but with $1/\epsilon = 0$ and b_{ij} substituted by $b_{ij} - 2C_F \delta_{ij}$. Inserting these finite quantities in the matching condition, Eq. (18), one finds the Wilson coefficients in the form

$$C_i(\mu) = \left(\delta_{ij} + \frac{\alpha_s}{4\pi} f_{ij} \ln \left(\frac{\Lambda^2}{\mu^2} \right) + O(\alpha_s^2) \right) C_j^{tree}, \quad (24)$$

where $C_i^{tree} = C_i(\mu = \Lambda)$ are the coefficients derived from a high scale model by integrating out heavy particles and neglecting the QCD corrections. In this formula f_{ij} are some numerical coefficients which explicit form is irrelevant for the present discussion. The above relation is shown in order to motivate the subsequent analysis needed to make contact with $0\nu\beta\beta$ scales, $\mu = \mu_0 \sim 100$ MeV. As seen Eq. (24) in this case contains a large logarithmic term $\alpha_s \ln(\Lambda/\mu_0)$ potentially dangerous for perturbation theory when $\Lambda \sim \Lambda_{LNV}$. The appearance of the large logarithms is inevitable issue of renormalizable theories, when one wants to relate the values of a physical quantity like C_i measured at two hierarchical scales like Λ_{LNV} and μ_0 . The way out is very well known: one has to sum up the large logarithms in all orders in α_s on the basis of the Renormalization Group Equations (RGE). It is done in what follows.

B. QCD running of Wilson coefficients

In the previous section we recalled a well-known fact that the effective operators may mix under renormalization since the operator renormalization constants Z_{ij} represent, in general, a non-diagonal matrix. It is introduced in Eq. (22) in order to eliminate the divergencies in the operator matrix elements Eq. (20). In practice it is convenient to reformulate the operator mixing in terms of the mixing of the corresponding Wilson coefficients. These two approaches are well-known to be equivalent [14, 15]. It might be helpful to remind this point and the main steps leading to the RGE for the Wilson coefficients.

Following Refs. [14, 15] we may consider the effective Lagrangian (2) within the conventional counterterm approach as a sum of the 4-quark-leg effective vertices $\mathcal{O}(q^{(0)})$ constructed of bare quark fields $q^{(0)}$ accompanied with bare ‘‘couplings’’ $C^{(0)}$ related to the renormalized ones

$$q^{(0)} = Z_q^{1/2} q, \quad C_i^{(0)} = Z_{ij}^C C_j. \quad (25)$$

Thus for the Lagrangian terms in Eq. (2) one can write

$$C_k^{(0)} \mathcal{O}_k(q^{(0)}) = Z_q^2 Z_{ij}^C C_j \mathcal{O}_i(q). \quad (26)$$

The amplitude calculated with this Lagrangian schematically takes the form

$$\text{Ampl.} \sim Z_q^2 Z_{ij}^C C_j \langle \mathcal{O}(q)_i \rangle^{(0)} = C_j \langle \mathcal{O}(q)_i \rangle. \quad (27)$$

The righthand side can be made finite by adjusting the renormalization constants. In practice it is done order by order in perturbation theory separating the above Lagrangian in the renormalized part and the counterterms $C_i \mathcal{O}(q)_i + c.t.$ The above result must be consistent with Eq. (22). Then $Z_{ij}^{(C)} = Z_{ij}^{-1}$. Using the fact that the bare quantities $C_i^{(0)}$ are independent of the renormalization scale μ

$$\frac{d}{d \ln \mu} C_i^{(0)} = \frac{d}{d \ln \mu} Z_{ij}^{-1} C_j = 0 \quad (28)$$

one finds the corresponding RGE for the Wilson coefficients in the matrix form

$$\frac{d\vec{C}(\mu)}{d \ln \mu} = \hat{\gamma}^T \vec{C}(\mu), \quad (29)$$

where $\vec{C} = (C_1, C_2, \dots)$ and the anomalous dimension matrix $\hat{\gamma}$ is defined as

$$\hat{\gamma} = \frac{1}{\hat{Z}} \frac{d}{d \ln \mu} \hat{Z}. \quad (30)$$

The LO expression in the $\overline{\text{MS}}$ -scheme is [15]:

$$\hat{\gamma}(\alpha_s) = -2\alpha_s \frac{\partial \hat{Z}_1(\alpha_s)}{\partial \alpha_s}, \quad (31)$$

where \hat{Z}_1 is the matrix factor of the singularity $1/\epsilon$ in Eq. (23). Thus we have in the LO approximation

$$\gamma_{ij}(\alpha_s) = \frac{\alpha_s}{4\pi} \gamma_{ij}, \quad \text{with} \quad \gamma_{ij} = -2(b_{ij} - 2C_F \delta_{ij}), \quad (32)$$

where γ_{ij} are the components of the anomalous dimension matrix $\hat{\gamma}$.

The solution of Eq. (29) can be represented in terms of the μ -evolution matrix

$$\vec{C}(\mu) = \hat{U}(\mu, \Lambda) \cdot \vec{C}(\Lambda). \quad (33)$$

between the low and high energy scales μ and Λ , respectively. In the LO one finds

$$\hat{U}(\mu, \Lambda) = \hat{V} \text{Diag} \left\{ \left[\frac{\alpha_s(\Lambda)}{\alpha_s(\mu)} \right]^{\gamma_i/(2\beta_0)} \right\} \hat{V}^{-1}. \quad (34)$$

The LO QCD running coupling constant is as usual

$$\alpha_s(\mu) = \frac{\alpha_s(\Lambda)}{1 - \beta_0 \frac{\alpha_s(\Lambda)}{2\pi} \log \left(\frac{\Lambda}{\mu} \right)} \quad (35)$$

with $\beta_0 = (33 - 2f)/3$, where f is the number of the quark flavors with masses $m_f < \mu$. For a normalization we use the experimental value $\alpha_s(\mu = M_z) = 0.118$ [26]. Eq. (34) contains the matrix \hat{V} defined as

$$\text{Diag} \{ \gamma_i \} = \hat{V}^{-1} \hat{\gamma} \hat{V}, \quad (36)$$

where $\hat{\gamma}$ is the matrix form of γ_{ij} , see Eq. (32). The matrix in the left hand side of Eq. (36) is a diagonal matrix with the diagonal elements γ_i . The same notation is used in Eq. (34).

The quark thresholds in the evolution of the $C_i(\mu)$ down to $\mu_0 \sim 1$ GeV can be approximately taken into account by the chain of the μ -evolution matrices with different numbers, f , of quark flavors:

$$\hat{U}(\mu, \Lambda = M_W) = \hat{U}^{(f=3)}(\mu_0, \mu_c) \hat{U}^{(f=4)}(\mu_c, \mu_b) \hat{U}^{(f=5)}(\mu_b, M_W), \quad (37)$$

$$\hat{U}(\mu, \Lambda > m_t) = \hat{U}^{(f=3)}(\mu_0, \mu_c) \hat{U}^{(f=4)}(\mu_c, \mu_b) \hat{U}^{(f=5)}(\mu_b, \mu_t) \hat{U}^{(f=6)}(\mu_t, \Lambda), \quad (38)$$

for two cases of the high energy scale Λ considered in the present paper. Here $\hat{U}^{(f)}$ are the matrix \hat{U} in Eq. (34) calculated for $f = 3, 4, 5, 6$ quark flavors. The intermediate scales we simply put to the corresponding quark thresholds $\mu_c = m_c, \mu_b = m_b, \mu_t = m_t$, which is an adequate appropriation for the LO analysis (for more details see Refs. [14, 15]).

C. Leading order QCD running of the $0\nu\beta\beta$ operator basis

In the leading order, the QCD corrections of the effective operators of the $0\nu\beta\beta$ basis (3)-(7) are shown in Fig. 3. Of course, other similar 1-loop diagrams with all other possible

gluon links of the quark legs have to be taken into account additionally. The diagrams (a), (b), (c) contribute to the operator matrix elements (20) with the following structures

$$(a) \sim (\bar{u}\Gamma^i P_X d) \cdot (\bar{u}\gamma_\alpha \gamma_\beta \Gamma^j \gamma^\beta \gamma^\alpha P_Y d) \cdot j_{\mathcal{O}} \cdot C_F \frac{1}{4} \frac{\alpha}{4\pi} \left(\frac{1}{\epsilon} + \log \frac{\mu^2}{-p^2} \right) \quad (39)$$

$$(b) \sim -(\bar{u}\Gamma^i \gamma_\sigma \gamma_\alpha T^a P_X d) \cdot (\bar{u}\Gamma^j \gamma^\sigma \gamma^\alpha T^a P_Y d) \cdot j_{\mathcal{O}} \cdot \frac{1}{4} \frac{\alpha}{4\pi} \left(\frac{1}{\epsilon} + \log \frac{\mu^2}{-p^2} \right) \quad (40)$$

$$(c) \sim (\bar{u}\Gamma^i \gamma_\sigma \gamma_\alpha T^a P_X d) \cdot (\bar{s}\gamma^\alpha \gamma^\sigma \Gamma^j T^a P_Y d) \cdot j_{\mathcal{O}} \cdot \frac{1}{4} \frac{\alpha}{4\pi} \left(\frac{1}{\epsilon} + \log \frac{\mu^2}{-p^2} \right), \quad (41)$$

where Γ^i are the Lorentz structures corresponding to the operators from Eqs. (3)-(7) with the leptonic currents $j_{\mathcal{O}}$, see Eq. (8) and T^a being the generators of $SU(N=3)$. Using Eq. (32) we find the LO anomalous dimensions for all the $0\nu\beta\beta$ -operators as

$$\hat{\gamma}_{(31)}^{XY} = -2 \begin{pmatrix} -\frac{3}{N} & -6 \\ 0 & 6C_F \end{pmatrix}, \quad \hat{\gamma}_{(12)}^{XX} = -2 \begin{pmatrix} 6C_F - 3 & \frac{1}{2N} + \frac{1}{4} \\ -12 - \frac{24}{N} & -3 - 2C_F \end{pmatrix} \quad (42)$$

$$\gamma_{(3)}^{XX} = -2 \left(\frac{3}{N} - 3 \right), \quad \gamma_{(5)}^{XY} = -3\gamma_{(4)}^{XY} = -12C_F, \quad (43)$$

$$\hat{\gamma}_{(45)}^{XX} = -2 \begin{pmatrix} 9 - 2C_F & 3i - \frac{6i}{N} \\ i + \frac{2i}{N} & 6C_F + 1 \end{pmatrix}, \quad (44)$$

where the superscripts $X \neq Y = L, R$ denote the chiralities while the subscripts indicate the operators from Eqs. (3)-(7) mixed under the renormalization. For instance, the first matrix mixes the operators $\mathcal{O}_3^{XY}, \mathcal{O}_1^{XY}$ with $X \neq Y = L, R$, and so on. The anomalous dimensions in the second row (43) are just numbers renormalizing each of the operators $\mathcal{O}_3^{XX}, \mathcal{O}_{5,4}^{XY}$ separately without mixing. Then, using Eqs. (34)-(37), one can find the μ -evolution matrix $U(\mu, \Lambda)$ and explicitly relate the Wilson coefficients at high- and low-energy scales Λ and μ , respectively.

V. QCD CORRECTED $0\nu\beta\beta$ HALF-LIFE AND LIMITS ON HIGH-SCALE MODELS

Now we express Eq. (9) in terms of the high-scale $C_i(\Lambda)$ Wilson coefficients using the RGE relations derived in the previous section and obtain the leading order QCD corrected $0\nu\beta\beta$ -decay half-life formula, which is *the central result* of the present paper:

$$\begin{aligned} \left[T_{1/2}^{0\nu\beta\beta} \right]^{-1} &= G_1 \left| \beta_1^{XX} (C_1^{LL}(\Lambda) + C_1^{RR}(\Lambda)) + \beta_1^{LR} (C_1^{LR}(\Lambda) + C_1^{RL}(\Lambda)) + \right. & (45) \\ &\quad \left. + \beta_2^{XX} (C_2^{LL}(\Lambda) + C_2^{RR}(\Lambda)) + \right. \\ &\quad \left. + \beta_3^{XX} (C_3^{LL}(\Lambda) + C_3^{RR}(\Lambda)) + \beta_3^{LR} (C_3^{LR}(\Lambda) + C_3^{RL}(\Lambda)) \right|^2 + \\ &+ G_2 \left| \beta_4^{XX} (C_4^{RR}(\Lambda) + C_4^{RR}(\Lambda)) + \beta_4^{LR} (C_4^{LR}(\Lambda) + C_4^{RL}(\Lambda)) + \right. \\ &\quad \left. + \beta_5^{XX} (C_5^{RR}(\Lambda) + C_5^{RR}(\Lambda)) + \beta_5^{LR} (C_5^{LR}(\Lambda) + C_5^{RL}(\Lambda)) \right|^2, \end{aligned}$$

where

$$\beta_1^{XX} = \mathcal{M}_1 U_{(12)11}^{XX} + \mathcal{M}_2 U_{(12)21}^{XX}, \quad \beta_1^{LR} = \mathcal{M}_3^{(+)} U_{(31)12}^{LR} + \mathcal{M}_1 U_{(31)22}^{LR}, \quad (46)$$

$$\beta_2^{XX} = \mathcal{M}_1 U_{(12)12}^{XX} + \mathcal{M}_2 U_{(12)22}^{XX}, \quad (47)$$

$$\beta_3^{XX} = \mathcal{M}_3^{(-)} U_{(3)}^{XX}, \quad \beta_3^{LR} = \mathcal{M}_3^{(+)} U_{(31)11}^{LR} \quad (48)$$

$$\beta_4^{XX} = -|\mathcal{M}_4| U_{(45)11}^{XX} + |\mathcal{M}_5| U_{(45)21}^{XX}, \quad \beta_4^{LR} = |\mathcal{M}_4| U_{(4)}^{LR}, \quad (49)$$

$$\beta_5^{XX} = -|\mathcal{M}_4| U_{(45)12}^{XX} + |\mathcal{M}_5| U_{(45)22}^{XX}, \quad \beta_5^{LR} = |\mathcal{M}_5| U_{(5)}^{LR}. \quad (50)$$

From Eqs. (3) and (5) one sees that \mathcal{O}_1^{XY} and \mathcal{O}_3^{XY} are symmetric under the interchange of X and Y . Consequently, in Eq. (45) $C_1^{LR} = C_1^{RL}$ and $C_3^{LR} = C_3^{RL}$, which is equivalent to a factor 2. Coherently with Eqs. (A.7)-(A.8) the subscripts of the evolution matrix U in the parenthesis denote the subscripts of the operators from Eqs. (3)-(7) mixed under the renormalization, the subscripts without the parenthesis specify the U -matrix element. Numerical values of these matrix elements are given in Appendix A. The nuclear matrix elements \mathcal{M}_i are defined in Ref. [4] and can be calculated in any nuclear structure model. We use their numerical values as given in Ref. [2] and display them for convenience in Table I.

${}^A\text{X}$	\mathcal{M}_1	\mathcal{M}_2	$\mathcal{M}_3^{(+)}$	$\mathcal{M}_3^{(-)}$	$ \mathcal{M}_4 $	$ \mathcal{M}_5 $
${}^{76}\text{Ge}$	9.0	-1.6×10^3	1.3×10^2	2.1×10^2	$ 1.9 \times 10^2 $	$ 1.9 \times 10^1 $
${}^{136}\text{Xe}$	4.5	-8.5×10^2	6.9×10^1	1.1×10^2	$ 9.6 \times 10^1 $	$ 9.3 $

TABLE I: The numerical values of the nuclear matrix elements \mathcal{M}_i taken from Ref. [2].

The currently best lower bounds on the $0\nu\beta\beta$ -decay half-life come from experiments using ${}^{76}\text{Ge}$ (combined GERDA and Heidelberg–Moscow limits) [10] and ${}^{136}\text{Xe}$ (combined EXO and KamlandZEN limits) [13]. We use:

$$T_{1/2}^{0\nu\beta\beta}({}^{76}\text{Ge}) \geq T_{1/2}^{0\nu\beta\beta\text{-exp}}({}^{76}\text{Ge}) = 3.0 \cdot 10^{25} \text{ yrs}, \quad (51)$$

$$T_{1/2}^{0\nu\beta\beta}({}^{136}\text{Xe}) \geq T_{1/2}^{0\nu\beta\beta\text{-exp}}({}^{136}\text{Xe}) = 3.4 \cdot 10^{25} \text{ yrs}. \quad (52)$$

From these experimental lower bounds we derive upper limits on $C_i(\Lambda_{1,2})$ for two scales $\Lambda_1 = M_W$ and $\Lambda_2 = \Lambda_{LNV} \sim 1 \text{ TeV}$ using Eq. (45). The choice of Λ_2 is motivated by the facts that the $d = 9$ effective operators (3)-(7), contributing to the short-range mechanism of $0\nu\beta\beta$, are generated at the mass scale of the heavy particles $\sim \Lambda_{LNV}$, which, considering the current LHC bounds, are heavier than $\sim 1 \text{ TeV}$. The results are shown in Table I, where we also present, for comparison, the “old limits” on C_i (cf. Refs. [2, 4]) neglecting the QCD running, but updated with the new half-life limits as given in Eqs (51) and (52). Note that neglecting the QCD running corresponds to setting $U_{ij}^{XY} = \delta_{ij}$ in Eqs. (46)-(50).

Deriving individual limits on C_i in Table I we assumed for simplicity that there are no significant cancellations between the terms in the right-hand side of Eq. (45). This is equivalent to assuming the dominance of only one C_i at a time. Comparing different numbers in Table I, one sees that the running between M_W and $\mu_0 \simeq 1 \text{ GeV}$ is more important than

the running between 1 TeV and M_W , but the latter is not negligible. As can also be seen from Table I, the QCD RGE running has the largest impact on the contributions to the operators \mathcal{O}_1^{XY} and \mathcal{O}_5^{XX} . This can be understood since in the RGE running they mix with the operators \mathcal{O}_2^{XY} and \mathcal{O}_4^{XX} , respectively, which have significantly larger nuclear matrix elements, as seen from Table I.

	With QCD		Without QCD	With QCD		Without QCD
A_X	$ C_1^{XX}(\Lambda_1) $	$ C_1^{XX}(\Lambda_2) $	$ C_1^{XX} $	$ C_1^{LR,RL}(\Lambda_1) $	$ C_1^{LR,RL}(\Lambda_2) $	$ C_1^{LR,RL} $
^{76}Ge	5.0×10^{-10}	3.8×10^{-10}	2.6×10^{-7}	1.5×10^{-8}	9.1×10^{-9}	2.6×10^{-7}
^{136}Xe	3.4×10^{-10}	2.6×10^{-10}	1.8×10^{-7}	9.7×10^{-9}	6.1×10^{-9}	1.8×10^{-7}
A_X	$ C_2^{XX}(\Lambda_1) $	$ C_2^{XX}(\Lambda_2) $	$ C_2^{XX} $	–	–	–
^{76}Ge	3.5×10^{-9}	5.2×10^{-9}	1.4×10^{-9}	–	–	–
^{136}Xe	2.4×10^{-9}	3.5×10^{-9}	9.4×10^{-10}	–	–	–
A_X	$ C_3^{XX}(\Lambda_1) $	$ C_3^{XX}(\Lambda_2) $	$ C_3^{XX} $	$ C_3^{LR,RL}(\Lambda_1) $	$ C_3^{LR,RL}(\Lambda_2) $	$ C_3^{LR,RL} $
^{76}Ge	1.5×10^{-8}	1.6×10^{-8}	1.1×10^{-8}	2.0×10^{-8}	2.1×10^{-8}	1.8×10^{-8}
^{136}Xe	9.7×10^{-9}	1.1×10^{-8}	7.4×10^{-9}	1.4×10^{-8}	1.4×10^{-8}	1.2×10^{-8}
A_X	$ C_4^{XX}(\Lambda_1) $	$ C_4^{XX}(\Lambda_2) $	$ C_4^{XX(0)} $	$ C_4^{LR,RL}(\Lambda_1) $	$ C_4^{LR,RL}(\Lambda_2) $	$ C_4^{LR,RL(0)} $
^{76}Ge	5.0×10^{-9}	3.9×10^{-9}	1.2×10^{-8}	1.7×10^{-8}	1.9×10^{-8}	1.2×10^{-8}
^{136}Xe	3.4×10^{-9}	2.7×10^{-9}	7.9×10^{-9}	1.2×10^{-8}	1.3×10^{-8}	7.9×10^{-9}
A_X	$ C_5^{XX}(\Lambda_1) $	$ C_5^{XX}(\Lambda_2) $	$ C_5^{XX} $	$ C_5^{LR,RL}(\Lambda_1) $	$ C_5^{LR,RL}(\Lambda_2) $	$ C_5^{LR,RL} $
^{76}Ge	2.3×10^{-8}	1.4×10^{-8}	1.2×10^{-7}	3.9×10^{-8}	2.8×10^{-8}	1.2×10^{-7}
^{136}Xe	1.6×10^{-8}	9.5×10^{-9}	8.2×10^{-8}	2.8×10^{-8}	2.0×10^{-8}	8.2×10^{-8}

TABLE II: Individual upper limits on the Wilson coefficients $C_i(\Lambda)$ in Eq. (45) calculated for two matching scales, $\Lambda_1 = M_W$ and $\Lambda_2 = \Lambda_{LNV} = 1$ TeV, using the experimental bounds (51), (52). Here $X = L, R$. For comparison we also give limits on the C_i , without the QCD running. We highlighted with boldface text those positions where the QCD running leads to about 3 orders (for C_1^{XX}), one order (for $C_1^{LR,RL}$) of magnitude and a factor 3–4 (for $C_4^{XX}, C_5^{LR,RL}$) effect.

If one is interested in constraining a particular high-scale model one should directly use Eq. (45) retaining only those coefficients C_i , which are present in the model. The corresponding limits on the model parameters in certain cases can be significantly modified with respect to their values given in Table I, which, as we mentioned above, are based on the hypothesis about one coefficient dominance at a time. In the case of a particular model this assumption may not be valid. For example, the model specified in Eqs. (13), (16) contains simultaneously two non-vanishing Wilson coefficients at the matching scale, $C_1^{RR}(\Lambda)$ and $C_2^{RR}(\Lambda)$, which obey the relation $C_2^{RR} = (3/20)C_1^{RR}$. Using Eqs. (45)-(50) one finds for $C_1^{RR}(\Lambda)$ nearly the same limit as in Table I, but due to the above mentioned relation the limit on $C_2(\Lambda)$ turns out to be $C_2^{RR}(\Lambda_2) = (3/20)(C_1^{RR} < 3.8 \times 10^{-10}) < 5.7 \times 10^{-11}$, which is two orders of magnitude stronger than the individual limit $C_2^{RR}(\Lambda_2) < 5.2 \times 10^{-9}$ given in Table I for the case of ^{76}Ge . For all models listed in [9] one can find QCD improved limits

in the same manner.

VI. CONCLUSIONS

In this paper we have calculated QCD corrections to the complete list of Lorentz-invariant operators for the short-range (SR) part of the $0\nu\beta\beta$ -decay amplitude. We have used the RGE technique to derive 1-loop improved limits on all the Wilson coefficients appearing in the SR contributions to $0\nu\beta\beta$ -decay. We stress again, that we have taken special care to present our results in such a way, that improved limits can be derived easily, should updated experimental limits or improved nuclear physics calculations become available.

Our numerical results show that the QCD corrections are indeed important. We note that both more and less stringent limits can result from taking into account QCD corrections, depending on the operator under consideration. In particular, the appearance of color mismatched operators lead to operator mixing which, due to largely different nuclear matrix elements for different operators, can lead to surprisingly large changes in some limits. QCD improved limits from $0\nu\beta\beta$ -decay should therefore be used, when comparing constraints from $0\nu\beta\beta$ -decay with those derived from LHC.

Acknowledgements

M.G. thanks the IFIC for hospitality during her stay. This work was supported by the Spanish MICINN grants FPA2014-58183-P and Multidark CSD2009-00064 (MINECO), and PROMETEOII/2014/084 (Generalitat Valenciana), and by Fondecyt (Chile) under grants 1150792 and 3160642.

I. APPENDIX A. EXPLICIT FORM OF THE RGE EVOLUTION MATRIX.

Here we give the numeric values of the RGE μ -evolution matrix elements defined in Eq. (34) and taking into account the quark thresholds according to (37), (38). In the notations used in Eqs. (46)-(50) we have for two reference values, $\Lambda_1 = M_W$ and $\Lambda_2 = 1$ TeV, of the high energy scale Λ , and $\mu_0 = 1$ GeV, the following results

$$\hat{U}_{(12)}^{XX}(\mu_0, \Lambda_1) = \begin{pmatrix} 1.88 & 0.06 \\ -2.76 & 0.40 \end{pmatrix}, \quad U_{(3)}^{XX}(\mu_0, \Lambda_1) = 0.76, \quad (\text{A.1})$$

$$\hat{U}_{(31)}^{LR}(\mu_0, \Lambda_1) = \begin{pmatrix} 0.87 & -1.40 \\ 0 & 2.97 \end{pmatrix}, \quad \hat{U}_{(45)}^{XX}(\mu_0, \Lambda_1) = \begin{pmatrix} 2.33 & 0.39i \\ 0.64i & 3.35 \end{pmatrix}, \quad (\text{A.2})$$

$$U_{(4)}^{LR}(\mu_0, \Lambda_1) = 0.70, \quad U_{(5)}^{LR}(\mu_0, \Lambda_1) = 2.97. \quad (\text{A.3})$$

and

$$\hat{U}_{(12)}^{XX}(\mu_0, \Lambda_2) = \begin{pmatrix} 2.24 & 0.07 \\ -3.70 & 0.27 \end{pmatrix}, \quad U_{(3)}^{XX}(\mu_0, \Lambda_2) = 0.70, \quad (\text{A.4})$$

$$\hat{U}_{(31)}^{LR}(\mu_0, \Lambda_2) = \begin{pmatrix} 0.84 & -2.19 \\ 0 & 4.13 \end{pmatrix}, \quad \hat{U}_{(45)}^{XX}(\mu_0, \Lambda_2) = \begin{pmatrix} 2.98 & 0.69i \\ 1.15i & 4.82 \end{pmatrix}, \quad (\text{A.5})$$

$$U_{(4)}^{LR}(\mu_0, \Lambda_2) = 0.62, \quad U_{(5)}^{LR}(\mu_0, \Lambda_2) = 4.13. \quad (\text{A.6})$$

Using these RGE evolution matrix elements one can calculate the corresponding β_i^{XY} -coefficients (46)-(50) for values of the nuclear matrix elements \mathcal{M}_i other than we give in Table I and used for the derivation of the limits presented in Table I.

-
- [1] I. Avignone, Frank T., S. R. Elliott, and J. Engel, Rev.Mod.Phys. **80**, 481 (2008), arXiv:0708.1033.
- [2] F. F. Deppisch, M. Hirsch, and H. Päs, J.Phys. **G39**, 124007 (2012), arXiv:1208.0727.
- [3] H. Päs, M. Hirsch, H. Klapdor-Kleingrothaus, and S. Kovalenko, Phys.Lett. **B453**, 194 (1999).
- [4] H. Päs, M. Hirsch, H. Klapdor-Kleingrothaus, and S. Kovalenko, Phys.Lett. **B498**, 35 (2001), arXiv:hep-ph/0008182.
- [5] K. Babu and R. Mohapatra, Phys.Rev.Lett. **75**, 2276 (1995), arXiv:hep-ph/9506354.
- [6] M. Hirsch, H. Klapdor-Kleingrothaus, and S. Kovalenko, Phys.Lett. **B372**, 181 (1996), arXiv:hep-ph/9512237.
- [7] H. Päs, M. Hirsch, and H. Klapdor-Kleingrothaus, Phys.Lett. **B459**, 450 (1999), arXiv:hep-ph/9810382.
- [8] M. Hirsch, H. Klapdor-Kleingrothaus, and S. Kovalenko, Phys.Rev. **D54**, 4207 (1996), arXiv:hep-ph/9603213.
- [9] F. Bonnet, M. Hirsch, T. Ota, and W. Winter, JHEP **1303**, 055 (2013), arXiv:1212.3045.
- [10] GERDA Collaboration, M. Agostini et al., Phys.Rev.Lett. **111**, 122503 (2013), arXiv:1307.4720.
- [11] EXO-200 Collaboration, J. Albert et al., Nature **510**, 229234 (2014), arXiv:1402.6956.
- [12] KamLAND-Zen Collaboration, I. Shimizu, Neutrino 2014, Boston (2014).
- [13] KamLAND-Zen Collaboration, A. Gando et al., Phys. Rev. Lett. **110**, 062502 (2013), arXiv:1211.3863.
- [14] G. Buchalla, A. J. Buras, and M. E. Lautenbacher, Rev.Mod.Phys. **68**, 1125 (1996), arXiv:hep-ph/9512380.
- [15] A. J. Buras, Weak Hamiltonian, CP violation and rare decays, Probing the standard model of particle interactions. Proceedings, Summer School in Theoretical Physics, NATO Advanced Study Institute, 68th session, Les Houches, France, July 28-September 5, 1997. Pt. 1, 2, pp. 281-539, 1998, arXiv:hep-ph/9806471.
- [16] N. Mahajan, Phys.Rev.Lett. **112**, 031804 (2014).

- [17] T. Peng, M. J. Ramsey-Musolf, and P. Winslow, (2015), arXiv:1508.04444.
- [18] M. Doi, T. Kotani, and E. Takasugi, Prog.Theor.Phys.Suppl. **83**, 1 (1985).
- [19] K. Muto, E. Bender, and H. Klapdor, Z.Phys. **A334**, 187 (1989).
- [20] A. Faessler, M. González, S. Kovalenko, and F. Simkovič, Phys.Rev. **D90**, 096010 (2014), arXiv:1408.6077.
- [21] J. Hyvriinen and J. Suhonen, Phys.Rev. **C91**, 024613 (2015).
- [22] J. Menendez, A. Poves, E. Caurier, and F. Nowacki, J.Phys.Conf.Ser. **312**, 072005 (2011).
- [23] M. Blennow, E. Fernandez-Martinez, J. Lopez-Pavon, and J. Menendez, JHEP **1007**, 096 (2010), arXiv:1005.3240.
- [24] R. Sen'kov and M. Horoi, Phys.Rev. **C90**, 051301 (2014), arXiv:1411.1667.
- [25] Private communication of F. Simkovič, 2015.
- [26] Particle Data Group, J. Beringer *et al.*, Phys.Rev. **D86**, 010001 (2012).
- [27] A. J. Buras, M. Misiak and J. Urban, Nucl. Phys. B **586**, 397 (2000) doi:10.1016/S0550-3213(00)00437-5 [hep-ph/0005183].

Erratum: QCD running in neutrinoless double beta decay: Short-range mechanisms

In the summation of the one-loop QCD corrections to the short-range mechanism of neutrinoless double beta decay, analyzed in Ref. [1], we lost a minus sign in the case of the anomalous dimensions of some effective short-range operators.

Then two of our anomalous dimension matrices have to be modified. For this reason the upper limits on the C_1^{XX} , C_2^{XX} , C_4^{XX} and C_5^{XX} Wilson coefficients have to be updated. This erratum doesn't modify the main conclusions of this work.

- Equation (42) has to be replaced by

$$\hat{\gamma}_{(31)}^{XY} = -2 \begin{pmatrix} -\frac{3}{N} & -6 \\ 0 & 6C_F \end{pmatrix}, \quad \hat{\gamma}_{(12)}^{XX} = -2 \begin{pmatrix} 6C_F - 3 & -\frac{1}{2N} + \frac{1}{4} \\ -12 - \frac{24}{N} & -3 - 2C_F \end{pmatrix} \quad (\text{A.7})$$

Comment: In reference [2], the anomalous dimension matrix $\gamma_{(12)}^{XX}$ was also calculated. We agree with their results, as can be seen after inserting the definition of C_F . However, in this paper a different convention for the $\sigma_{\mu\nu}$ matrix was used. While in [2] they use $\sigma_{\mu\nu} = \frac{1}{2}[\gamma_\mu, \gamma_\nu]$, in our paper we use $\sigma_{\mu\nu} = \frac{i}{2}[\gamma_\mu, \gamma_\nu]$. This is the reason why in [2] there is a extra minus sign in the off-diagonal elements of $\gamma_{(12)}^{XX}$.

- Equation (44) has to be replaced by

$$\hat{\gamma}_{(45)}^{XX} = -2 \begin{pmatrix} -3 - 2C_F & -3i - \frac{6i}{N} \\ -i + \frac{2i}{N} & 6C_F - 3 \end{pmatrix}, \quad (\text{A.8})$$

- The upper limits on Wilson coefficients C_1^{XX} , C_2^{XX} , C_4^{XX} and C_5^{XX} have to be updated. The updated Table II is the following:
- In the Appendix, Equation (A1) has to be updated by

$$\hat{U}_{(12)}^{XX}(\mu_0, \Lambda_1) = \begin{pmatrix} 1.95 & 0.01 \\ -2.82 & 0.45 \end{pmatrix}, \quad U_{(3)}^{XX}(\mu_0, \Lambda_1) = 0.76, \quad (\text{A.9})$$

- In the Appendix, Equation (A2) has to be updated by

$$\hat{U}_{(31)}^{LR}(\mu_0, \Lambda_1) = \begin{pmatrix} 0.87 & -1.40 \\ 0 & 2.97 \end{pmatrix}, \quad \hat{U}_{(45)}^{XX}(\mu_0, \Lambda_1) = \begin{pmatrix} 0.45 & -0.70i \\ -0.05i & 1.95 \end{pmatrix}, \quad (\text{A.10})$$

$A\text{X}$	$ C_1^{XX}(\Lambda_1) $	$ C_1^{XX}(\Lambda_2) $	$ C_1^{XX(0)} $	$ C_1^{LR,RL}(\Lambda_1) $	$ C_1^{LR,RL}(\Lambda_2) $	$ C_1^{LR,RL(0)} $
^{76}Ge	4.9×10^{-10}	3.6×10^{-10}	2.6×10^{-7}	1.5×10^{-8}	9.1×10^{-9}	2.6×10^{-7}
^{136}Xe	3.3×10^{-10}	2.5×10^{-10}	1.8×10^{-7}	9.7×10^{-9}	6.1×10^{-9}	1.8×10^{-7}
$A\text{X}$	$ C_2^{XX}(\Lambda_1) $	$ C_2^{XX}(\Lambda_2) $	$ C_2^{XX(0)} $	–		
^{76}Ge	3.1×10^{-9}	4.0×10^{-9}	1.4×10^{-9}	–		
^{136}Xe	2.1×10^{-9}	2.7×10^{-9}	9.4×10^{-10}	–		
$A\text{X}$	$ C_3^{XX}(\Lambda_1) $	$ C_3^{XX}(\Lambda_2) $	$ C_3^{XX(0)} $	$ C_3^{LR,RL}(\Lambda_1) $	$ C_3^{LR,RL}(\Lambda_2) $	$ C_3^{LR,RL(0)} $
^{76}Ge	1.5×10^{-8}	1.6×10^{-8}	1.1×10^{-8}	2.0×10^{-8}	2.1×10^{-8}	1.8×10^{-8}
^{136}Xe	9.7×10^{-9}	1.1×10^{-8}	7.4×10^{-9}	1.4×10^{-8}	1.4×10^{-8}	1.2×10^{-8}
$A\text{X}$	$ C_4^{XX}(\Lambda_1) $	$ C_4^{XX}(\Lambda_2) $	$ C_4^{XX(0)} $	$ C_4^{LR,RL}(\Lambda_1) $	$ C_4^{LR,RL}(\Lambda_2) $	$ C_4^{LR,RL(0)} $
^{76}Ge	2.6×10^{-8}	3.4×10^{-8}	1.2×10^{-8}	1.7×10^{-8}	1.9×10^{-8}	1.2×10^{-8}
^{136}Xe	1.8×10^{-8}	2.3×10^{-8}	7.9×10^{-9}	1.2×10^{-8}	1.3×10^{-8}	7.9×10^{-9}
$A\text{X}$	$ C_5^{XX}(\Lambda_1) $	$ C_5^{XX}(\Lambda_2) $	$ C_5^{XX(0)} $	$ C_5^{LR,RL}(\Lambda_1) $	$ C_5^{LR,RL}(\Lambda_2) $	$ C_5^{LR,RL(0)} $
^{76}Ge	1.6×10^{-8}	1.2×10^{-8}	1.2×10^{-7}	3.9×10^{-8}	2.8×10^{-8}	1.2×10^{-7}
^{136}Xe	1.1×10^{-8}	8.1×10^{-9}	8.2×10^{-8}	2.8×10^{-8}	2.0×10^{-8}	8.2×10^{-8}

- In the Appendix, Equation (A4) has to be updated by

$$\hat{U}_{(12)}^{XX}(\mu_0, \Lambda_2) = \begin{pmatrix} 2.39 & 0.02 \\ -3.83 & 0.35 \end{pmatrix}, \quad U_{(3)}^{XX}(\mu_0, \Lambda_2) = 0.70, \quad (\text{A.11})$$

- In the Appendix, Equation (A5) has to be updated by

$$\hat{U}_{(31)}^{LR}(\mu_0, \Lambda_2) = \begin{pmatrix} 0.84 & -2.19 \\ 0 & 4.13 \end{pmatrix}, \quad \hat{U}_{(45)}^{XX}(\mu_0, \Lambda_2) = \begin{pmatrix} 0.35 & -0.96i \\ -0.06i & 2.39 \end{pmatrix} \quad (\text{A.12})$$

-
- [1] M. González, M. Hirsch and S. G. Kovalenko, Phys. Rev. D **93**, no. 1, 013017 (2016) doi:10.1103/PhysRevD.93.013017 [arXiv:1511.03945 [hep-ph]].
- [2] A. J. Buras, M. Misiak and J. Urban, Nucl. Phys. B **586**, 397 (2000) doi:10.1016/S0550-3213(00)00437-5 [hep-ph/0005183].